

Constrained Object Placement Using Reinforcement Learning

Benedikt Kreis Nils Dengler Jorge de Heuvel Rohit Menon Hamsa Datta Perur Maren Bennewitz

Abstract—Close and precise placement of irregularly shaped objects requires a skilled robotic system. Particularly challenging is the manipulation of objects that have sensitive top surfaces and a fixed set of neighbors. To avoid damaging the surface, they have to be grasped from the side, and during placement, their neighbor relations have to be maintained. In this work, we train a reinforcement learning agent that generates smooth end-effector motions to place objects as close as possible next to each other. During the placement, our agent considers neighbor constraints defined in a given layout of the objects while trying to avoid collisions. Our approach learns to place compact object assemblies without the need for predefined spacing between objects as required by traditional methods. We thoroughly evaluated our approach using a two-finger gripper mounted to a robotic arm with six degrees of freedom. The results show that our agent outperforms two baseline approaches in terms of object assembly compactness, thereby reducing the needed space to place the objects according to the given neighbor constraints. On average, our approach reduces the distances between all placed objects by at least 60 %, with fewer collisions at the same compactness compared to both baselines.

I. INTRODUCTION

Object manipulation, particularly picking and placing, is a highly researched field in robotics [1] [2] [3] [4]. Different applications lead to a variety of challenges such as limited workspace, tight tolerances affecting error margins, object quantity, and shape diversity. Thus, one of the main problems to be solved is the precise positioning of objects at target poses [5], which is especially difficult when the items cannot be grasped from the top, e.g., with a suction gripper, due to sensitive surfaces, necessitating side grasping. This scenario arises in sectors such as electronics production, automotive manufacturing, or also archaeology in the reconstruction of historical artifacts.

The aforementioned challenges can partially be tackled by dense packing methods [6] [7]. However, current work in this field has its limitations and does not consider, e.g., adjacent relations between objects or the need for sufficient space for the gripper’s operation due to the side-grasping restriction. Furthermore, existing methods do not strictly follow a given assembly sequence of the objects to be placed to keep adjacent relations between neighbors and minimize deviation from it.

In this paper, we propose a reinforcement learning (RL) approach to enable a robotic manipulator to place objects

All authors are with the Humanoid Robots Lab, University of Bonn, Germany. Nils Dengler, Jorge de Heuvel, and Maren Bennewitz are additionally with the Lamarr Institute for Machine Learning and Artificial Intelligence, Bonn, Germany. This work has partly been funded by the European Union’s HORIZON 2020 research and innovation programme under grant agreement n°964854. Corresponding author: kreis@cs.uni-bonn.de

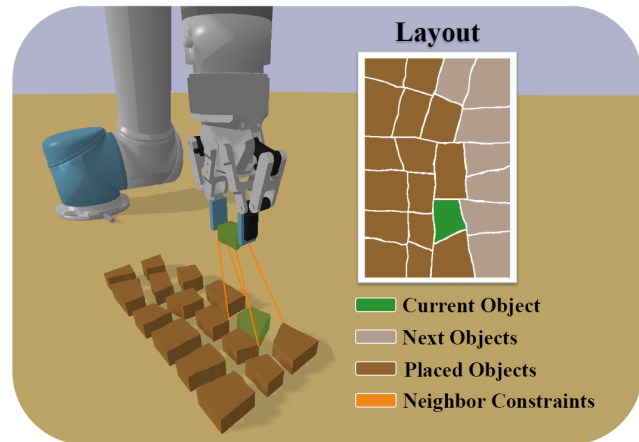


Fig. 1: Using our RL approach, the robotic manipulator places an exemplary assembly in its workspace. The goal is to place all objects as compact as possible while considering the objects’ constraining neighbor relations.

closely together according to a layout that defines neighbor constraints between the objects. Our approach learns to maximize the resulting assembly compactness as well as the number of collisions between the objects and the gripper. From an initial grasping position, our agent tries to place an arbitrary shaped object as close as possible to its desired position according to a given layout while considering neighbor constraints to previously placed objects. Furthermore, after successfully placing the object, it retracts the gripper from the placement position while avoiding further collisions with objects in its vicinity. By design, our RL agent is able to handle sub-optimal grasps resulting from arbitrary yaw rotations of the object during the picking process.

Fig. 1 shows our agent in the process of placing an exemplary assembly by controlling the robotic manipulator, in this case, a 6-DoF robotic arm with a two-finger gripper. As can be seen, the robot effectively inserts one object into the assembly, thereby minimizing the distances to the previously placed neighbor objects. As our experimental results show, our approach varies the gaps between the objects depending on their shape, consequently reducing the distances between all objects by at least 60 % on average, with fewer collisions compared to two baseline approaches.

To summarize, the main contributions of our work are:

- A model-free RL framework to learn smooth arm and end effector (EE) motions for precise object placement, accounting for neighbor constraints and minimizing neighbor distances while trying to avoid collisions.
- A qualitative and quantitative evaluation compared to two baseline methods that demonstrate the performance of our approach in terms of assembly compactness.

II. RELATED WORK

Research in pick-and-place (P&P) manipulation involves a broad spectrum ranging from the entire P&P pipeline to specific tasks such as object grasping and stacking [8], [9], [10], [11]. The exploration of deep learning techniques, such as reinforcement learning, brought significant advances to this domain [1], [2]. Yet, the distinct task of positioning objects side by side, similar to dense packing, has been considered less frequently in the literature. Our work bridges this gap by introducing an RL approach that optimizes object placement under consideration of given neighbor constraints.

In the field of self-supervised learning for precise object placement, Berscheid *et al.* [5] presented a method that combines learning primitives with one-shot imitation learning to align objects according to a visual input. Zhang *et al.* [4] demonstrated the effectiveness of deep Q-learning in stacking cuboids side by side, exploiting the uniformity of the cuboids for simplified grasping and placement. Our approach extends these works by learning to optimize the placement of objects to minimize distances between them and increase the spatial efficiency of object assemblies.

Dense packing and the peg-in-a-hole task represent benchmarks for assessing the precision and efficiency of P&P manipulations. Studies in dense packing often simplify the complexity of the task by focusing on heuristic and reinforcement learning strategies for fitting objects within limited spaces, without fully addressing diverse object shapes and gripper spatial requirements [6], [7]. Our work diverges by emphasizing the importance of maintaining relative positions among objects, thereby addressing a crucial aspect overlooked in prior research. Furthermore, the peg-in-a-hole task, known for its tight tolerances, contrasts with our methodology, which seeks to avoid collisions entirely, ensuring a delicate balance between precision and object integrity [12].

Integrating affordance maps and neural radiance fields into placement tasks has opened new avenues for specifying preferred placement locations. However, these methods often fall short in dictating or optimizing the relational positioning of objects based on adjacency constraints [13]. Our method surpasses these limitations by ensuring compact object placement, which is pivotal for tasks requiring the arrangement of objects at tight distances from one another.

Our method improves on existing methodologies by learning to precisely place objects close to each other while avoiding collisions. This overcomes the limitations of existing work in accommodating diverse object shapes, optimizing space utilization, and maintaining specific relational arrangements among placed objects.

III. PROBLEM DEFINITION

We consider the following problem: In a tabletop environment, a robotic arm has to place irregularly shaped objects according to a given layout containing constraints that define neighbor relations. We assume the usage of a two-finger end effector, moving in four dimensions (x, y, z, θ) . Since we control the EE, the robotic arm can be of any degree

of freedom (DoF). Our RL agent has to determine the best incremental movement $(\Delta x, \Delta y, \Delta z, \Delta \theta)$ of the EE at each time step to move the current object with the EE as fast as possible to the best pose according to the constraints defined in the object layout. Thereby, the closer the objects are placed to each other the better, while collisions should be avoided. Note that due to the necessary side-grasping, the agent has to leave space to allow a collision-free opening of the gripper. We assume the order in which the objects are placed can be derived from the given layout using a simple heuristic and that all object poses can be reliably estimated.

In the following, we distinguish between three types of objects: *Layout Objects*, which have not been grasped yet; the *Placing Object*, which has been grasped for placing; and *Table Objects*, which have been placed at their final position on the table workspace.

IV. OUR APPROACH

Since the optimal spacing between objects for tight and collision-free placement is unknown, we propose an RL system that learns to place each object as close as possible to its neighbors according to the layout, while avoiding collisions with the objects and the gripper.

As we focus on the placing action, for grasping, we use an automated routine that selects grasp poses according to simple heuristics. In this way, our agent learns to place objects as best as possible, even with sub-optimal grasp poses. Fig. 2 shows an overview of our approach. Following the assembly sequence extracted from the layout, our agent tries to place an arbitrarily shaped object closely to its neighbors that have been previously placed. In the following sections, we introduce our approach in more detail.

A. Object Neighbor Concepts

To support the learning of our system, we introduce two concepts that guide the agent to place objects close to each other. First, we calculate the corresponding corners $c_i \in N_c$ on adjacent object polygons in the layout to constrain the placement of neighboring objects. Each c_i corresponds to the outer-most points of shared edges between neighboring objects (see Fig. 2 a). Furthermore, to align the objects in the workspace, we define two reference lines (l_x, l_y) located at the assembly's x and y axis to align objects along them (see Fig. 2 b). Both concepts are used for further computations in the reward function.

B. RL Task Description

During an episode, the goal of the agent is to place an object on the table, as shown in Fig. 1. Furthermore, each episode is divided into four task states $q \in [0, 3]$ as depicted in Fig. 2 c. Task states 1-3 are integrated into the RL architecture while task state 0 is executed by a predefined grasping routine.

At the beginning of each training episode ($q=0$), a random object of the layout is selected as placing object o_n and the robot is set to an initial configuration above the workspace.

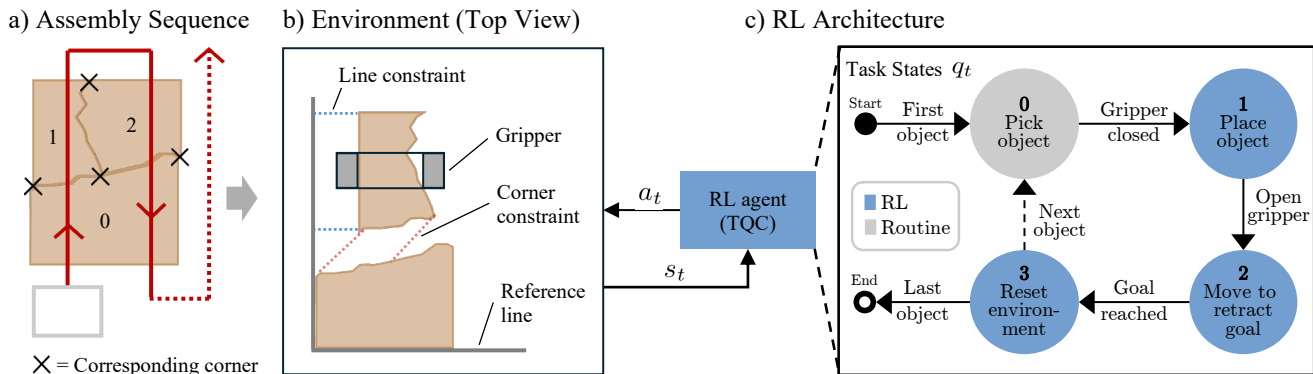


Fig. 2: Overview of our approach. a) The assembly sequence is determined by sliding a virtual window with a fixed size in a snake-like pattern (red line) over the layout. Furthermore, the corresponding corners are determined by searching for the two most distant points between all shared object edges in the layout. b) The exemplary environment depicts two objects from a top-down view. The bottom one, has been already placed along the reference lines and the next one in the assembly sequence is between the gripper fingers. To maneuver the grasped object close to its neighbors, the RL agent uses the corresponding corners to calculate the corner and the line constraints. c) At each time step t , the RL agent observes the state of the environment s_t and sends action commands a_t to the EE. During one episode, the agent passes through four internal task states 0-3. Note that task state 0 is not learned, but executed by an automated routine.

Given the assembly sequence, we spawn all preceding objects o_1, \dots, o_{n-1} on the table to simulate a successful placement of them. Both, the yaw angle of o_n (θ_{place}) and the EE’s yaw angle (θ_{EE}) are randomly chosen according to ($\theta_{\text{place}}, \theta_{\text{EE}} \in [-90^\circ, +90^\circ]$). Afterwards, the agent has to place the object as close as possible to the ones on the table ($q=1$). Since we consider the retraction of the EE after placing the objects ($q=2$) as part of the pipeline, we use a retraction goal that it has to reach to successfully terminate the episode, while avoiding contact with any object on the table. An episode terminates unsuccessfully when the maximum number of steps N_{ep} is reached, or a collision occurs. When an episode terminates, we reset the environment ($q=3$) and the agent starts again in task state 0.

Note that during training, only single object placements are considered, and those objects are randomly sampled. During inference, we extend the task to place all objects sequentially according to the given assembly sequence.

C. RL Architecture

In general, RL optimizes transitions from one state to the next $s_t \rightarrow s_{t+1}$ following the Markov Decision Process. The reward $r_t = r(s_t, a_t)$ describes the incentive for the RL agent to take an action $a_t = \pi_\phi(s_t)$ at time step t with respect to a policy π_ϕ . Typically, states and actions are summarized in pairs of tuples (s_t, a_t, r_t, s_{t+1}) . The objective is to maximize

TABLE I: Observation space.

Observation	Notation	Task State	Size
Corresponding corner distances	$(x, y, z)_c$	1	36
Distances to reference lines	$(x, y, z)_r$	1	12
EE pose	$(x, y, z, \theta)_{\text{EE}}$	1-3	4
Retract goal	$(x, y, z)_g$	2	3
Placing object orientation	θ_{obj}	1	1
Reference line object Boolean	l	1	1
Task state	q	0-3	1
	Sum		58

the cumulative return $R = \sum_{i=t}^T \gamma^{(i-t)} r_t$ of the γ -discounted rewards.

RL Algorithm: In this work, we use the off-policy algorithm Truncated Quantile Critics (TQC) [14] with two critics and 25 quantiles. To ensure sufficient exploration, we add Gaussian noise from a process \mathcal{N} with a standard deviation σ_{ϵ_π} to the actions, so that $a_t = \pi_\phi(s_t) + \mathcal{N}(0, \sigma_{\epsilon_\pi})$.

Action Space: At each time step our agent computes the next incremental action $(\Delta x, \Delta y, \Delta z, \Delta \theta)$ for the robot’s EE. Additionally, the agent decides when to open the gripper. All actions are normalized to values in the interval $[-1, +1]$.

Observation Space: The complete observation space is shown in Tab. I. As described in Sec. IV-B and illustrated by Fig. 2c, at each time step our system can be in one of four possible states $q \in [0, 3]$. Depending on q , unavailable or irrelevant parts of the observations, in the current state are padded with 0 (see Tab. I). Note that the partial vector sizes for corresponding corner distances ($N_{c,\text{max}}$) and distances to reference lines ($N_{l,\text{max}}$) are calculated by the maximum number of expected object neighbors ($\text{max}(N_o) = 6$). All observations are normalized to values on the interval $[0, +1]$.

D. Reward

The design of the reward function takes two main objectives into account. First, to improve the compactness of the assembly. Second, the object placement must be executed efficiently in terms of time, while avoiding collisions. All distances and angles used to calculate the rewards are normalized to values on the interval $[0, +1]$. The reward r consists of four components:

$$r = r_{q_1} + r_{q_1 \rightarrow 2} + r_{q_2} + r_{\text{col}} \quad (1)$$

The first three components depend on the task state q and the last one r_{col} is given in all task states to avoid collisions throughout the episode. That means per task state only two reward components are used by the agent while the remaining ones are set to 0. In the following paragraphs, we introduce all reward components in detail.

Object Placement: In task state 1, which is illustrated in Fig. 2 b, the agent has to place the given object in the environment. During this task state, the agent is penalized for time-inefficient solutions by the reward r_{q_1} , which incentivizes it to move the placing object as fast as possible towards its predecessor or a bordering reference line. Furthermore, the correct object orientation $\theta_{o_{\text{place}}}$ according to the layout $\theta_{o_{\text{layout}}}$ is ensured by the same reward defined as:

$$r_{q_1} = \underbrace{-\alpha_n \cdot (d_c + d_l)}_{\text{neighbor constraints}} - \underbrace{\alpha_\theta \cdot |\theta_{o_{\text{layout}}} - \theta_{o_{\text{place}}}|}_{\text{object angle difference}} \quad (2)$$

where d_c is the mean Euclidean distance of corresponding corner-corner pairs between the placing object ($o \in 1$) and all neighbor objects ($o \in 2, \dots, N_o$) that have been placed on the table. Respectively, d_l is the mean Euclidean distance of corresponding corner-line pairs between the placing object ($o \in 1$) and all reference lines (l_x, l_y). d_c is calculated with:

$$d_c = \frac{\sum_{o=2}^{N_o} \frac{\sum_{c=1}^{N_c} \|\vec{p}_{1,c} - \vec{p}_{o,c}\|}{N_c}}{N_o} \quad (3)$$

where the vector $\vec{p} = \begin{pmatrix} x \\ y \\ z \end{pmatrix}$ describes a corner point c in 3D space and N_c is the amount of corresponding corners per object, which is object dependent. d_l is calculated in the same manner by treating the reference line as a virtual object. The corresponding corner on the line is defined by the shortest point-to-line distance between corresponding corner on the placing object and the reference line.

Object Release: When the agent transits to the next task state ($q:1 \rightarrow 2$), the gripper is opened. At this time step, the agent receives the reward $r_{q_1 \rightarrow 2}$ defined as:

$$r_{q_1 \rightarrow 2} = \underbrace{\alpha_c \cdot [1 - \tanh(\beta_c \cdot d_c)] + \alpha_l \cdot [1 - \tanh(\beta_l \cdot d_l)]}_{\text{neighbor closeness}} - \underbrace{\alpha_d \cdot d_{\text{drop}}}_{\text{drop height}} \quad (4)$$

The left term incentivizes the agent to optimize the compactness of the assembly, while the right term ensures that the object is not dropped mid-air. It depends on the height d_{drop} during the release.

Gripper Retraction: After placing the object ($q=2$), the reward r_{q_2} , which is defined as:

$$r_{q_2} = \underbrace{-\alpha_m \cdot \|\vec{p}_{\text{drop}} - \vec{p}_{N_{\text{ep}}}\|}_{\text{object movement}} - \underbrace{\alpha_g \cdot \|\vec{p}_{\text{ret}} - \vec{p}_{\text{EE}}\|}_{\text{retract goal}} \quad (5)$$

ensures that the EE moves to the retract goal. It depends on the Euclidean distance between the retract goal \vec{p}_{ret} and the current EE position \vec{p}_{EE} . Once the object is placed, its further movement is prevented by the left term, which is dependent on the drop position \vec{p}_{drop} of the EE and its position at the end of the episode $\vec{p}_{N_{\text{ep}}}$.

Collision Avoidance: To avoid collisions, the agent is penalized for contacts between the *robot* and *table*, and between *robot* and table objects o_{table} , as well as the placing object o_{place} by the reward r_{col} defined as:

$$r_{\text{col}} = \begin{cases} -\alpha_{\text{col},o} & , \text{ if contact } o_{\text{place}} \leftrightarrow o_{\text{table}} \\ -\alpha_{\text{col},r} & , \text{ if contact } robot \leftrightarrow o_{\text{table}} \\ -\alpha_{\text{col},t} & , \text{ if contact } robot \leftrightarrow table \end{cases} \quad (6)$$

The collision conditions are also a termination criteria for the episode.

E. Learning Strategy

All relevant training parameters are listed in Tab. II. To accelerate training convergence, we gradually increase the difficulty of the learned task with a curriculum learning strategy by varying the EE position at the start of each training episode. In the first curriculum step, the EE is initialized 3 cm above the placing object position according to the layout. When the evaluation success is greater than 80 % the transition to the next curriculum step is triggered. In the last curriculum step, the EE is initialized centrally above the assembly at a height of $\frac{1}{4}$ of the arm's reach. Between the first and the last step of the curriculum, 20 intermediate steps are linearly interpolated. In the same manner, the gripper's retract height is gradually adapted between 3 cm to 8 cm. Without curriculum learning, the RL agent was not able to converge.

V. DATASET GENERATION

For training and evaluation on realistic data, we generate our object dataset, based on the exemplary application of fresco reconstruction. The dataset consists of fresco fragments with irregular shapes as shown in Fig. 1. For the generation, we assume that archaeological frescoes can be abstracted as jigsaw puzzles. Harel and Ben-Shahar [15] create puzzles by cutting through a global polygonal shape with an arbitrary number of straight cuts. This method generates solely convex polygons. We adapt this idea to generate fresco fragments that are realistic in terms of dimensions, shape, and mass.

To use the generated fragments with common robot simulators such as PyBullet [16], we generate 3D CAD models. Additionally, the generator computes the assembly sequence by sliding a window with a fixed size in a snake pattern over the 2D fresco polygons (see Fig. 2 a). When a fragment is within the window it is added to the sequence. The method is similar to bottom-left nesting algorithms in dense packing [17].

TABLE II: Notations and Training settings.

Notation	Value	Description
N_{ep}	50	Maximum number of steps per episode
N_{crit}	2	Number of critics
B_E	$1 \cdot 10^5$	Experience replay buffer size
B_G	128	Minibatch size for each gradient update
l	$1 \cdot 10^{-3}$	Learning rate
γ	0.95	Discount factor
σ_{ϵ_π}	0.1	Std. deviation of exploration noise ϵ_π
τ	0.05	Soft update coefficient

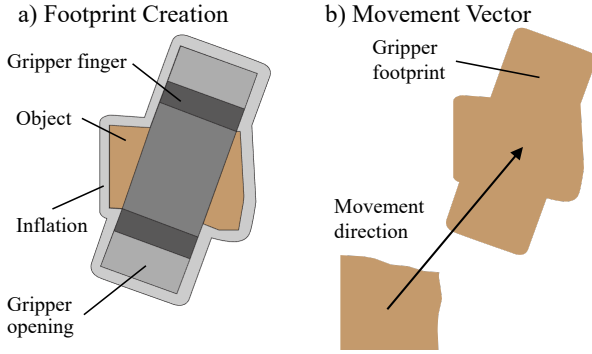


Fig. 3: a) We attach the required operation space of the gripper to the placing objects’ shape and create their union. The union is inflated to create a safety margin for the placement. The resulting shape is the gripper footprint. b) Baseline 2 uses the gripper footprint to plan suitable placement locations.

VI. EXPERIMENTAL EVALUATION

To demonstrate the performance of our RL approach in terms of efficient object placement, i.e., positional and angular displacement relative to the original layout as well as collisions, we provide the results of our qualitative and quantitative analysis, and we compare the performance of our system with two baseline approaches. In all experiments, the task of our agent is to sequentially perform the placement of a complete fresco assembly. More details are shown in the supplementary video¹.

A. Experimental Setup

For the experiments we use the 6-DoF robotic arm UR5, equipped with the two-finger gripper Robotiq 2F-85, as shown in Fig. 1. However, our approach is applicable to any robotic arm, since our agent learns EE movement increments, and it does not directly learn to control the robot’s joint angles. For all experiments, we rely on the TQC implementation of Stable-Baselines3 [18] and the OpenAI Gym toolkit [19], as well as PyBullet [16] for simulation. The actor and critic networks are implemented using three-layered fully-connected networks of size $\{128, 128, 128\}$. The training and evaluation are performed on a desktop computer equipped with an i9-11900KF CPU, 64 GB RAM, and an RTX 3080Ti GPU with 12 GB VRAM. While training, the agent handles only one fresco object. During evaluation instead, we extend the task to 100 unseen frescoes to show the agent’s generalization capabilities to unseen object shapes. Our agent trained using the reward scaling factors listed in Tab. III.

B. Baseline Approaches

To the best of our knowledge, there is no other work that focuses explicitly on the constrained placement of objects, as explained in Sec. IV. Therefore, we compare our RL approach (OUR), to a variation of our approach without reference lines (NO-L), and to two baselines (BL1 and BL2), which are explained below. To receive comparable results among all approaches, we assign a randomly generated grasp yaw angle $\theta_g \in [-90^\circ, +90^\circ]$ to each object. During

all experiments, θ_g is used to grasp the respective object. For action execution of each baseline, we use an inverse kinematics pipeline to generate collision-free motions to the placement targets computed by the baselines.

Baseline 1: For BL1, we generate equal gaps between all objects and check during execution if the gap size is sufficient. For this purpose, we iteratively increase the scale of the complete layout by $\alpha_b = 0.1$ and try to place each unscaled object at the shifted position resulting from the scaling. Compared to the original layout, the updated one has gaps between all objects. The gap size depends on the magnitude of α_b . As long as collisions occur during the placement, the process is repeated. Fig. 4b shows an exemplary placement result of BL1. As can be seen, BL1 results in an equally spaced assembly with larger gaps than necessary, due to the unique shapes of the objects.

Baseline 2: In contrast to BL1, the main idea of BL2 is not to equally increase the layout’s size, but to generate individual gaps between the current object and already placed table objects, to increase the compactness of the assembly. Therefore, we add the space required to open the gripper to the shape of the placing object, as shown from a top-down view in Fig. 3a. Then, the two shapes are unified and inflated to add a safety margin. Fig. 3b shows the resulting shape called the gripper footprint. The footprint is initially placed next to the preceding table object according to the assembly sequence. If any shapes overlap in this step, we calculate a movement vector \vec{m} to shift the current gripper footprint out of the collision. Given the footprint’s centroid C_p and all centroids of the colliding shapes $C_{col,n}$, we calculate the movement vector \vec{m} as follows:

$$\vec{m} = i \cdot \sum_{n=1}^{N_{col}} \frac{C_p - C_{col,n}}{\|C_p - C_{col,n}\|} \quad (7)$$

where i is the increment step, n is the shape number, and N_{col} is the number of collision shapes. The footprint is moved until no shapes overlap anymore, and a suitable placement location is found, as shown in Fig. 3b. For execution, all objects are sequentially placed on the table. Fig. 4d depicts an exemplary placement result of BL2.

C. Qualitative Results

Fig. 4 a-d shows the qualitative results of the experiments. Our RL-based approach demonstrates a refined balance between neighbor constraints and object geometry, resulting in a spatially optimized arrangement. In contrast, BL1 scales the layout uniformly, resulting in a functional, but less space-efficient configuration. Due to the individual spacing of BL2, this baseline results in the least compact representation, with larger gaps compared to BL1. Finally, NO-L, which does not include reference lines, highlights the significance of these guiding lines in achieving structured layouts. The absence of

TABLE III: Scaling factors used for the evaluation.

$\alpha_n = 0.1$	$\alpha_m = 0.5$	$\alpha_c = 3$	$\alpha_l = 6$	$\alpha_d = 0.5$	$\alpha_{col,o} = 2$
$\alpha_\theta = 0.1$	$\alpha_g = 0.1$	$\beta_c = 3$	$\beta_l = 3$	$\alpha_{col,l} = 1$	$\alpha_{col,r} = 2$

¹Video: <https://youtu.be/eQ9u2zKFeIQ>

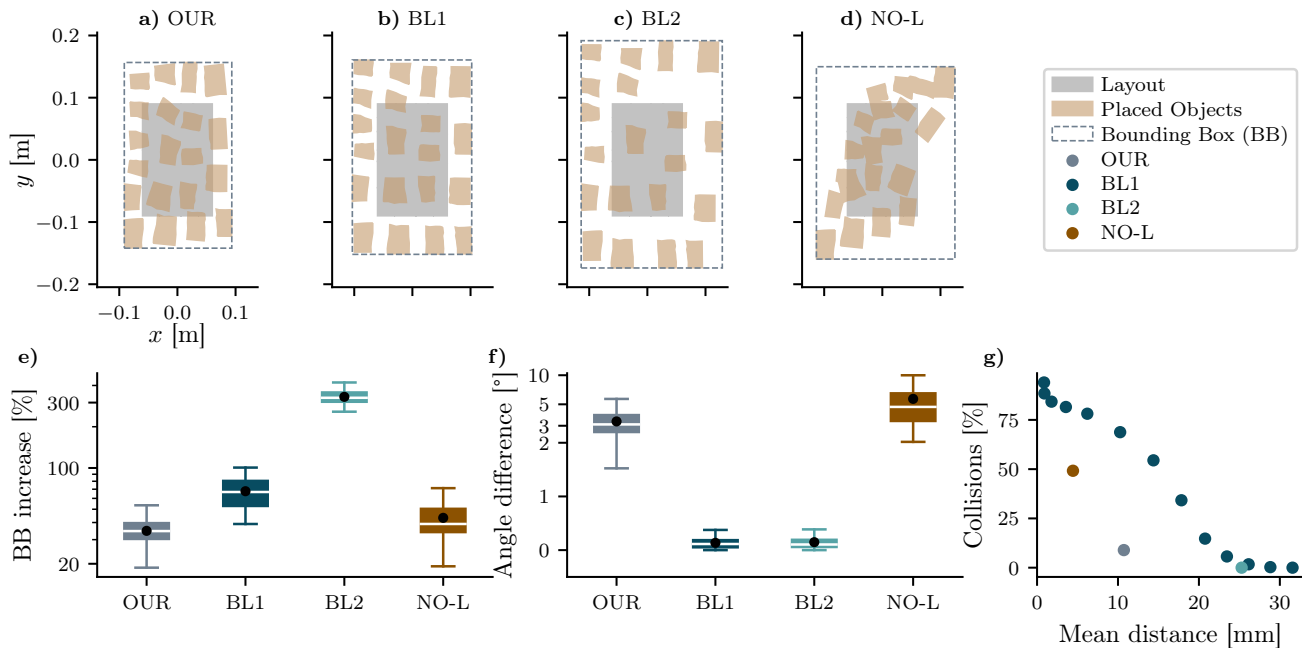


Fig. 4: The plots show all results of the qualitative and quantitative evaluation. a-d) Fresco assemblies are depicted from a 2D top-down view as abstracted polygons. a) Using our RL approach results in the most compact assembly. b) Scaling the fresco according to BL1 results in a larger bounding box due to the equal spacing. c) Scaling the objects relative to each other, according to BL2, results in the highest displacement. d) Without the reference lines, there is a clear object shift, highlighting the necessity of their use. e-g) The plots show the results of the quantitative evaluation as discussed in Sec. VI-D e) Our approach has the smallest bounding box increase compared to both baselines. f) The angle difference of both baselines is smaller than our approach. g) Our approach achieves the smallest mean object distance at a reasonable collision rate.

TABLE IV: Results of the quantitative evaluation.

Metric	OUR	BL1	BL2	NO-L
BB [%]	34.78 ± 6.88	67.68 ± 14.33	330.46 ± 37.86	43.27 ± 15.48
Angle [°]	3.32 ± 1.17	0.14 ± 0.11	0.15 ± 0.13	5.69 ± 3.28
Dist. [mm]	10.73 ± 1.64	26.22 ± 2.36	25.28 ± 2.04	4.44 ± 1.28
Coll. [%]	8.92 ± 7.44	0.00 ± 0.00	0.00 ± 0.00	49.18 ± 10.23

reference lines causes a shift in the overall layout due to the missing alignment functionality for the agent, which results in the propagation of relative placement errors.

In summary, these results show that while the baseline methods provide a foundation for object placement, the inclusion of RL and reference lines in our approach significantly improves spatial arrangement by considering neighbor constraints.

D. Quantitative Results

By evaluating our approach against the baselines, we used three different metrics to measure assembly efficiency, based on averages obtained from 100 assemblies. Specifically, the mean object distance is determined by the minimum centroid distances between all table objects. The mean circular angle difference measures the difference between the object angles defined in the layout and all placed fragments. Finally, the bounding box increase is defined as the difference between the sum of the bounding box area of all placed table fragments and the layout area divided by the layout area.

The results are shown in Tab. IV and Fig. 4 e-g. Our approach shows a significant reduction of the bounding box area, reaching only an increase of $34.78\% \pm 6.88$, resulting

in a more compact placement of the layout. In particular, our approach significantly reduces the bounding box expansion compared to BL1 (48%) and BL2 (89%). Fig. 4 g shows the same tendency for the mean distance between placed objects, strengthening our claim of the beneficial use of RL approaches for placement, due to the superior space utilization.

While the angle difference in our method is larger than that of the baselines (see Fig. 4 f), it is still within a range to sufficiently ensure a compact placement of all objects. However, this compactness comes with a trade-off in collision rates: Our method experienced a higher collision rate compared to the baselines, indicating a potential area for refinement in future iterations of our work. Nevertheless, the balance between mean distance and collision rate in our approach suggests an advantageous trade-off for applications where compactness is a priority, as shown in Fig. 4 g.

Furthermore, while our RL approach achieves commendable compactness and a minimal bounding box expansion of the layout, the absence of reference lines in the NO-L variant leads to a significant increase in collision rates and a slight decrease in placement accuracy. These results highlight the necessity of reference lines in our method to maintain a balance between compactness and operational feasibility, and it illustrates their integral role for a successful object placement.

VII. CONCLUSION

In this work, we presented a novel reinforcement learning-based method for the precise placement of irregularly shaped

objects in environments with constrained neighbor relations, demonstrating significant improvements in compactness and spatial efficiency over existing baselines. Our approach ensures minimized bounding box increase, significantly lower than the baseline methods, and it maintains dense object assemblies, achieving a notable reduction in mean distances between objects. Despite a higher collision rate in certain scenarios, the trade-offs are justifiable given the significant gains in compactness and space utilization. The implementation of reference lines proves to be a key factor in achieving these results, suggesting their essential role in structured and efficient object placement.

REFERENCES

- [1] A. Lobbezoo, Y. Qian, and H.-J. Kwon, "Reinforcement Learning for Pick and Place Operations in Robotics: A Survey," *Robotics*, vol. 10, no. 3, p. 105, 2021.
- [2] K. Kleeberger, R. Bormann, W. Kraus, and M. F. Huber, "A Survey on Learning-Based Robotic Grasping," *Current Robotics Reports*, vol. 1, no. 4, pp. 239–249, 2020.
- [3] A. X. Lee, C. Devin, Y. Zhou, T. Lampe, K. Bousmalis, J. T. Springenberg, A. Byravan, A. Abdolmaleki, N. Gileadi, D. Khosid, C. Fantacci, J. E. Chen, A. Raju, R. Jeong, M. Neunert, A. Laurens, S. Saliceti, F. Casarini, M. Riedmiller, R. Hadsell, and F. Nori, "Beyond Pick-and-Place: Tackling Robotic Stacking of Diverse Shapes," 2021.
- [4] J. Zhang, W. Zhang, R. Song, L. Ma, and Y. Li, "Grasp for Stacking via Deep Reinforcement Learning," in *2020 IEEE International Conference on Robotics and Automation (ICRA)*, 2020, pp. 2543–2549.
- [5] L. Berscheid, P. Meißner, and T. Kröger, "Self-Supervised Learning for Precise Pick-and-Place Without Object Model," *IEEE Trans. on Robotics (T-RO)*, vol. 5, no. 3, pp. 4828–4835, 2020.
- [6] F. Wang and K. Hauser, "Dense Robotic Packing of Irregular and Novel 3D Objects," *IEEE Transactions on Robotics*, vol. 38, no. 2, pp. 1160–1173, 2022.
- [7] H. Ren and R. Zhong, "An Autonomous Ore Packing system through Deep Reinforcement Learning," *Advances in Space Research*, p. S0273117724001273, 2024.
- [8] S. Liu, T. Tang, W. Zhang, J. Cui, and X. Xu, "A Brief Review of Recent Hierarchical Reinforcement Learning for Robotic Manipulation," in *2022 10th International Conference on Information Systems and Computing Technology (ISCTech)*, 2022, pp. 721–728.
- [9] I. J. Park, H. Han, J. Cho, and J. H. Park, "Knowledge-Based Reinforcement Learning for Industrial Robotic Assembly," in *2023 14th International Conference on Information and Communication Technology Convergence (ICTC)*, 2023, pp. 1684–1689.
- [10] A. Orsula, S. Bøgh, M. Olivares-Mendez, and C. Martinez, "Learning to Grasp on the Moon from 3D Octree Observations with Deep Reinforcement Learning," in *2022 IEEE/RSJ International Conference on Intelligent Robots and Systems (IROS)*, 2022, pp. 4112–4119.
- [11] F. Ceola, E. Maiettini, L. Rosasco, and L. Natale, "A Grasp Pose is All You Need: Learning Multi-fingered Grasping with Deep Reinforcement Learning from Vision and Touch," 2023.
- [12] S. Kim and A. Rodriguez, "Active Extrinsic Contact Sensing: Application to General Peg-in-Hole Insertion," 2022.
- [13] Z. He, N. Chavan-Daffe, J. Huh, S. Song, and V. Isler, "Pick2Place: Task-Aware 6DoF Grasp Estimation Via Object-Centric Perspective Affordance," in *Proc. of the IEEE Intl. Conf. on Robotics & Automation (ICRA)*, 2023.
- [14] A. Kuznetsov, P. Shvechikov, A. Grishin, and D. Vetrov, "Controlling Overestimation Bias with Truncated Mixture of Continuous Distributional Quantile Critics," in *Proceedings of the 37th International Conference on Machine Learning*, 2020, pp. 5556–5566.
- [15] P. Harel and O. Ben-Shahar, "Crossing cuts polygonal puzzles: Models and Solvers," in *2021 IEEE/CVF Conference on Computer Vision and Pattern Recognition (CVPR)*, 2021, pp. 3083–3092.
- [16] E. Coumans and Y. Bai, "PyBullet, a Python module for physics simulation for games, robotics and machine learning," <http://pybullet.org>, 2016.
- [17] S. Q. Xie, G. G. Wang, and Y. Liu, "Nesting of two-dimensional irregular parts: An integrated approach," *International Journal of Computer Integrated Manufacturing*, vol. 20, no. 8, pp. 741–756, 2007.
- [18] A. Raffin, A. Hill, A. Gleave, A. Kanervisto, M. Ernestus, and N. Dormann, "Stable-Baselines3: Reliable Reinforcement Learning Implementations."
- [19] G. Brockman, V. Cheung, L. Pettersson, J. Schneider, J. Schulman, J. Tang, and W. Zaremba, "OpenAI Gym," 2016.